Magnetic shielding of long paraboloid structures in the inhomogeneous magnetic field

J Kvitkovic[1,4], K Burnside[1,3], M Zhang[2] and S Pamidi[1,3]

[1] Center for Advanced Power Systems, Florida State University, Tallahassee, Florida 32310, USA
[2] Department of Electronic and Electrical Engineering, University of Strathclyde, Glasgow, UK
[3] Department of Electrical and Computer Engineering, FAMU-FSU College of Engineering, Tallahassee, Florida, USA
[4] Applied Superconductivity Center, National High Magnetic Field Laboratory, Florida State University, Tallahassee, 32310 Florida, USA

E-mail: kvitkovic@caps.fsu.edu

Abstract. Shielding efficacy of the high-temperature superconducting (HTS) magnetic shields depends on the superconductor properties and on the orientation of the external magnetic field. For precise magnetic field measurements in areas with changing direction of magnetic noise it is important to reduce both the parallel and perpendicular components of the magnetic field. We have designed and fabricated magnetic shields of 25 cm long paraboloid shape with closed sides from second-generation HTS tapes. We have characterized HTS shields in DC and variable frequency AC magnetic fields at 77 K above a copper electromagnet acting as the source of inhomogeneous magnetic noise. The HTS magnetic shields reduce the magnetic field noise penetration and enhance the sensitivity of magnetic field sensors. The measurements were performed with the magnetic shield placed between the noise source and the sensor. 2D finite element analysis using Comsol model was generated and the results were compared with the experimental data of magnetic field dependences of the shielding factor (SF).

1. Introduction

The properties of magnetic screens made of various high-temperature superconductors such as Bi-2223, Bi-2212, YBCO, and MgB_2 in the form of sheets, coils, tubes, cups or open slit tapes have been studied by researches for several years [1 - 6]. Using a Bi-2212 bulk tube and YBCO tape together to improve the shielding factors in DC and AC magnetic fields are also promising. Experiments on the magnetic properties of HTS superconducting screens and structures made of different compositions are usually performed in homogeneous axial or transverse external magnetic fields.

In shielding studies, inhomogeneous magnetic fields are rarely present. The sensitive measurement equipment affected by the magnetic field of a source localized in its vicinity also senses an inhomogeneous magnetic field due to screens. The concentration of the magnetic field by metallic construction parts reduces the screening properties and is complicated to locate.

In a time-varying external magnetic field, the flux line pinning allows screening currents to flow at the edges of the superconductor, forming a flux free region in the center. If the superconductor has a tube shape, then the inner surface has a region where the magnetic field is zero or strongly attenuated.

Characterization of the magnetic screen involves evaluation of the maximum magnetic field that can be shielded with the required value of the shielding factor. This maximum magnetic field is coupled with the maximum shielding currents that flow in the superconductor which are equal to the critical current of the superconductor.

HTS tapes are useful for screening DC and low-frequency magnetic fields. Very high-frequency magnetic fields can be easily screened by highly conductive metals using skin effect in the frequency range up to 10 kHz. At low frequency, the magnetic screening of HTS depends on the frequency of the applied magnetic field. This dependence is caused by the magnetic relaxation, which is coupled to the nonlinear relationship between the shielding currents represented by current density, J, and the electric field, E, in the simplified power-law formula $E \sim J^n$. A detailed knowledge of the E(J) characteristic of the superconductor is very important in the order to determine how the frequency of the applied magnetic field influences the magnetic shielding factor. It is practical to combine magnetization and transport measurements on the same sample, as the electric field induced in low-frequency magnetic measurements is usually much smaller than the electric field produced by transport current measurements [1].

Fagnard proposed to combine magnetic and transport measurements to determine the E(J) characteristic of Bi-2212 bulk tubes. He showed that Bi-2212 hollow cylinders could be used as very efficient magnetic shields, especially at temperatures below 60 K where their critical current exceeds the critical current of Bi-2223 bulk tubes. The temperature dependence of the critical current was determined from magnetic shielding experiments. It was shown that at a temperature of 10 K, the Bi-2212 sample can shield 1 T, a very high value of the magnetic field [1].

Shielding properties of a bulk Bi-2212 hollow cylinder with two axial slits, which cut the cylinder in equal halves, were studied in [2]. The cylinder was subjected to a transverse magnetic field at several angles. Results show that the slits block the shielding current flow and act as an input for the magnetic field. Fagnard reduced FEM model input parameters to critical current density, J_c, and a power-law exponent, n. They both were modeled as field-independent since the use of material data increases solving time [2].

Several different structures of magnetic shields made of YBCO coated conductors were studied experimentally in [3]. A slit is made along the centerline of a YBCO tape. This slit is then pulled apart to create a loop. Several loops were prepared from YBCO tape where shielding currents can flow without passing the resistive joint. The magnetic shield was placed to an axial DC magnetic field. The shielding factor was improved by reducing the gap, increasing number of layers, and for geometries with high aspect ratios [3].

The shielding factor of the superconducting magnetic shield made of two different superconducting HTS materials was tested in [4]. The outer section consists of rings formed of YBCO-123 tapes, which are capable of attenuating AC magnetic fields that reduce the magnetic field value on the inner bulk cylinder of Bi-2223 material, which provides complete shielding below its full penetration field. By using the additional YBCO rings on a Bi-2223 bulk cylinder, the shielding factor of the whole system increased considerably from 17 % to 87 % at 33 Hz and 10 mT [4].

The DC magnetic shielding factor of one-axis and three-axis stacks of short-circuited YBCO tape slits were described in [5]. The orientation of the external magnetic field was changed from the axial to the transverse direction. The applied magnetic field generates supercurrents in the tapes which formed the magnetic field whose orientation was opposite and parallel to the stack axis. The shielding factor in the direction of the applied field parallel to tape was very low which depends on the shape of each loop, the number of the loops in the stack and thickness of the superconductor layer. The weak performances were explained by the gap between both stacks of each axis and, by the small aspect ratios of the individual stacks [5].

Magnetic shielding properties of a bulk Bi-2223 superconducting tube in an inhomogeneous magnetic field generated by a solenoidal coil were presented in [6]. It was found that superconductor shielding properties in an inhomogeneous magnetic field are strongly dependent on source and sensor

position. A finite element model based on H-formulation using magnetic field-dependent critical current was developed [6].
We performed our previous magnetic shielding studies with YBCO tapes of various geometries as sheets and coils in DC and AC homogeneous magnetic fields in parallel and perpendicular orientations [8] - [16].

In this paper, we present the results of our experiments with a long paraboloid shield made of YBCO edge soldered sheets with dimensions 25 x 25 cm^2 in an inhomogeneous magnetic field. Soldered and non-soldered tapes in sidewalls and various configurations of the superconducting YBCO tapes were tested. We searched for configurations that provided the highest shielding factor with the lowest frequency dependence. Our study focused on reducing external magnetic field noise in the vicinity of sensitive magnetic field sensors using a long paraboloid shield.

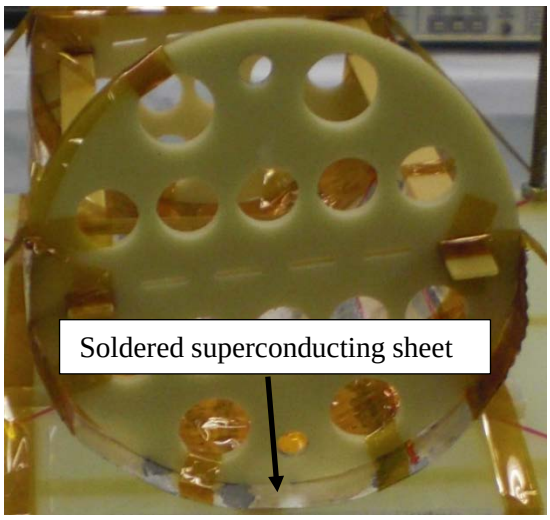

Figure 1. The G10 former for the long paraboloid magnetic shield.

Figure 2. One-layer soldered 25 x 25 cm^2 superconducting sheet.

2. Experimental

Long paraboloid samples were prepared by soldering commercial YBCO tapes supplied by American Superconductor Corporation [7]. The critical current at 77 K and self-magnetic field of the 45 mm wide YBCO tape was around 1 kA.

The long paraboloid magnetic shields were tested in DC and AC magnetic fields up to 338 Hz in a liquid nitrogen bath at 77 K. We measured magnetic shielding factor as a function of the number of layers and soldered or non-soldered tapes in the sidewalls.

Brass rods and fiberglass-reinforced epoxy sheets (G10) supported the long paraboloid magnetic shields in the magnet. The sample holder consists of two circular G10 plates (diameter = 130 mm) separated by 230 mm and fixed with 250 mm long G10 strips, figure 1. The YBCO tape was cut into 45 mm x 250 mm sections and neighboring tapes were soldered together with 12 mm overlaps to form a 25 x 25 cm^2 superconducting sheet, figure 2. This sheet was wrapped around the G10 circular plates to make the bottom of the paraboloid, figure 3. Tape Pieces, 130 mm x 45 mm formed the sidewalls of the paraboloid shield. Earlier samples had unsoldered and later samples had soldered sidewalls to the bottom tapes, see Appendix. The tapes were soldered at 150^o C using a 52 % Indium and 48 % Tin solder. Finally, the sample holder was inserted into the top of the copper magnet, which was placed in a stainless-steel cryostat, and filled with liquid nitrogen.

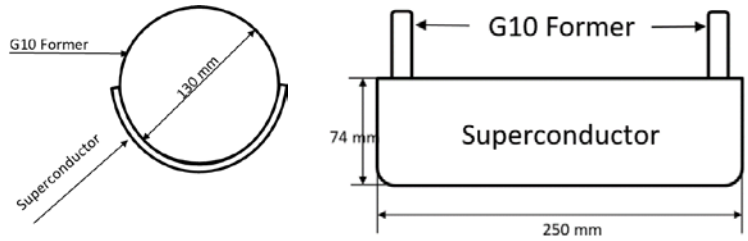

Figure 3. Simplified sketch of long paraboloid shield, left) side view and right) front view.

Figure 4. Photograph of the copper magnet.

The copper solenoid magnet served as the source of magnetic field noise for the shielding factor measurements, figure 4. The copper magnet consists of 171 turns in 3 layers wound from 2.6 mm copper wire onto a G10 bobbin. The coil height is 155 mm with an outer diameter of 410 mm producing a magnetic field in a large 400 mm diameter bore. The long paraboloid shields were placed in the inhomogeneous magnetic field region located above the magnet bore, figure 5. The external magnetic field had perpendicular and parallel components in various positions on the shield.

The signal from the AC/DC function generator Stanford Research Systems DS360 controlled the Techron AC/DC power supply current. A Tektronix A622 Current Probe measured the magnet current. In AC magnetic field experiments a series resonance and capacitor bank were used to reduce magnet impedance. For DC shielding factor measurements, a Keithley 2001 multimeter was used. For AC shielding factors a Lock-in amplifier Stanford Research Systems SR830 with a Keithley 2001 multimeter were utilized. Measurement details and the experimental set-up scheme are described in our previous paper [16].

The shielding factor (SF) was calculated using the external magnetic field - B_{ext} and the magnetic field at the Hall probe location in the long paraboloid - B_{HP} from the measurements by the following formula:

$$SF = \frac{B_{ext} - B_{HP}}{B_{ext}} * 100\ \% \qquad (1)$$

B_{HP} was measured using a calibrated cryogenic Hall probe [19], with the active area perpendicular to the magnet axis.

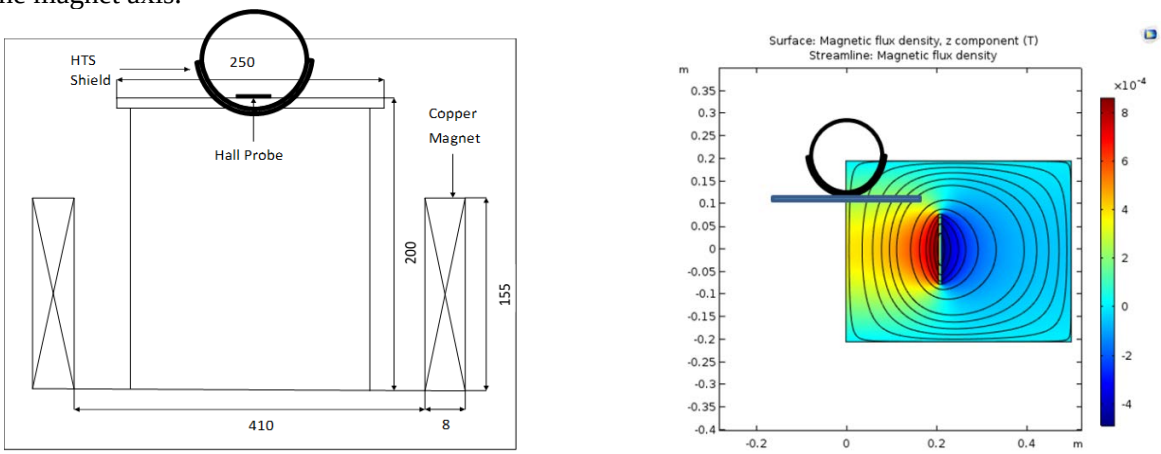

Figure 5. Left) Position of the long paraboloid shield above copper magnet. The distance between the Hall probe and the bottom of the HTS shield was 2 mm. Sketch is not to the scale. Right) Magnetic field at the shield location. Paraboloid structure is supported by the G10 board.

The center of the Hall sensor was positioned at the geometric center of the shield. The sample and the sensor were placed on the magnet axis, 4.5 cm above the edge of the copper solenoid magnet. A LakeShore 120 current source supplied an excitation current of 10 mA to the Hall probe.

3. 2D Comsol model

To study the shielding effect precisely, we developed a finite element model of the paraboloid shield. 2D H-formulation was used with the following equation [17]:

$$\mu_0\mu_r(\boldsymbol{H})\frac{\partial \boldsymbol{H}}{\partial t} + \mu_0 \boldsymbol{H}\frac{\partial \mu_r(\boldsymbol{H})}{\partial t} + \nabla \times (\rho \nabla \times \boldsymbol{H}) = 0 \qquad (2)$$

where magnetic field $H = [H_x, H_y]$ are the variables. The relative permeability, μ_r, for a non-magnetic substrate is constant, thus the second term on the left-hand side of Eq. (2) is zero. For the Ni-W substrate, in our samples, μ_r is a function of the applied magnetic field [17], therefore the value of the second term changes with time. The current density is $J=\nabla\times H$, and the electric field is $E=\rho I$. The resistivity, ρ, of HTS is calculated by the E-J power law, and the magnetic field-dependent critical current density of HTS is included using interpolation of the measured data [18].

The electrical field criterion $E_0 = 1$ μV/cm and an n-factor of 30, determined from tape I_c measurements, are applied to the simulation. The resistivities ρ of the non-superconducting subdomains are constants and defined by Ohm's law, $\rho = E/J$. To generate the external AC magnetic field, the Dirichlet boundary condition was used on the boundaries of the air domain:

$$H_y = B_{ext}/\mu_0 \sin(2\pi f t) \qquad (3)$$

where B_{ext} is the amplitude of AC magnetic field perpendicular to the wide face of the shield with frequencies f of 20 Hz and 293 Hz. Simulation results are plotted in figure 13.

4. Results and discussion

Shielding factors of the long paraboloid magnetic shield were measured as a function of magnetic field magnitude (all reported AC magnetic field values are RMS values), frequency, and the number of layers in the form of soldered layers made of YBCO superconducting tapes. All measurements were performed at a temperature of 77 K in a liquid nitrogen bath.

DC shielding factor dependencies for the 1-3 layer long paraboloid magnetic shield from soldered tapes without sidewalls on the DC magnetic field are plotted in figure 6. The shielding factor is 100 % below +/-1.35 mT above which SF decreases as magnetic field increases. A strong slope to 0% SF at +/- 5 mT is observed in the one-layer shield. At – 5mT, adding a second layer to the shield increases SF by 50% and adding a third layer increases the DC SF by an additional 14%. For the three-layer shield, SF remains at 100% up to +/- 2 mT, decreasing to 53% at +/- 10 mT.

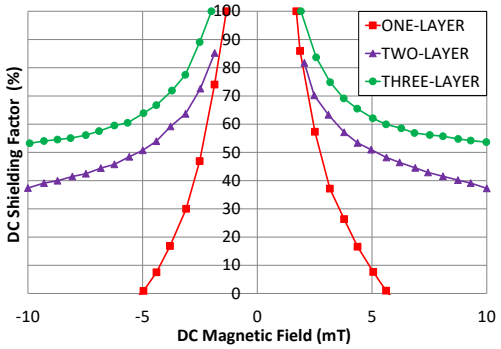

Figure 6. Measured DC shielding factor for a 1-3 layer soldered long paraboloid shield without sidewalls at 77 K.

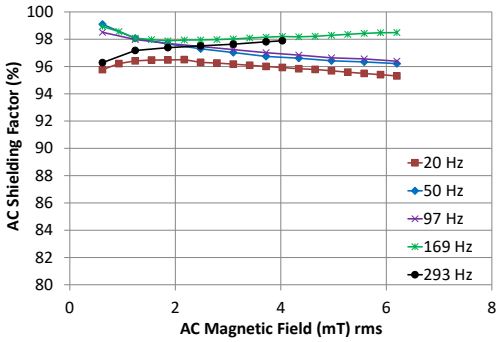

Figure 7. Measured AC shielding factor for a one-layer soldered long paraboloid shield at 20 – 293 Hz and 77 K.

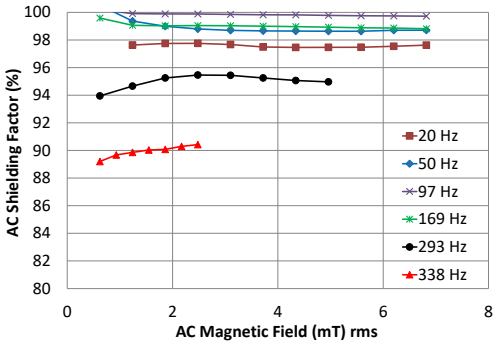

Figure 8. Measured AC shielding factor for a two-layer soldered long paraboloid shield at 20 – 338 Hz.

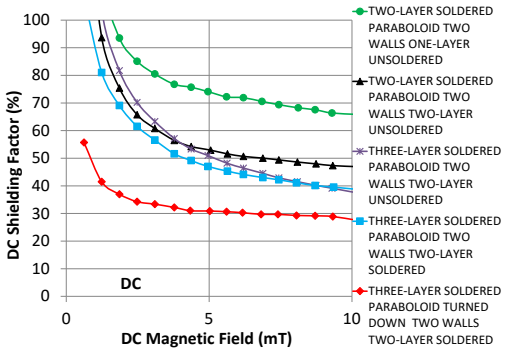

Figure 9. Measured Shielding factor comparison for various configurations with sidewalls in DC magnetic field.

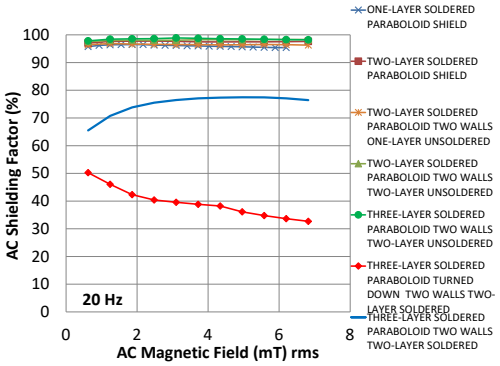

Figure 10. Measured Shielding factor comparison for various configurations in 20 Hz magnetic field.

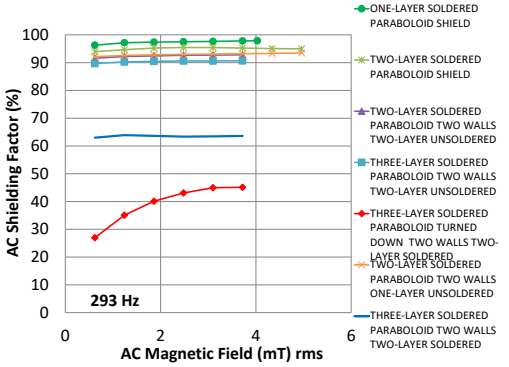

Figure 11. Measured Shielding factor comparison for various configurations in 293 Hz magnetic field.

The variation of AC shielding factor of the one-layer soldered paraboloid magnetic shield for frequencies 20 – 293 Hz is shown in figure 7. SF ranges from 95 – 99 % up to 6 mT rms. For lower B_{ext}, shielding factor increases with increasing frequency. The shielding factor decreases as B_{ext} increases. At 20 Hz, SF decreases from ~ 96.5 % to 95.4 % as B_{ext} increases from 1 mT to 6 mT. A similar trend is observed for other frequencies. Almost flat SF dependence is observed at 169 Hz between 2 and 5 mT. A maximum SF value of 99 % was seen in the one-layer soldered paraboloid shield.

Figure 8 depicts the SF in an AC magnetic field for the two-layer soldered paraboloid magnetic shield at 77 K. We obtained AC SF > 99 % for magnetic fields up to 7 mT at 97 Hz. At 20 Hz the SF rose to 98 % at 7 mT. We found that SF increased as the frequency of the magnetic field increased from 20 – 97 Hz and that SF has flat dependence up to 7 mT. Alternatively, SF decreased as frequency increased 97 – 338 Hz, due to temperature rise in the tapes accompanied by visible strong nitrogen bubbling.

Figure 9 compares the DC shielding factor magnetic field dependence of the soldered two and three-layer shields with unsoldered and soldered sidewalls. The two-layer soldered paraboloid shield with two sidewalls of unsoldered one-layer tape has the best DC shielding factor properties. The second best is the two-layer soldered paraboloid with two sidewalls of unsoldered two-layer tape. The three-layer soldered paraboloid magnetic shield with two walls of soldered two-layer tape turned down has the lowest DC SF. All curves have a similar shape, SF drops with an increase in the DC magnetic field.

For AC comparisons we performed our experiments at two frequencies 20 and 293 Hz. A maximum AC SF of 99 % at 20 Hz was achieved with the three-layer soldered paraboloid with two walls of two-layer unsoldered tape turned up in magnetic fields up 6 mT, see figure 10. The lowest AC SF ranging

from 33% to 50% is given by the three-layer soldered paraboloid magnetic shield with two walls of two-layer soldered tape turned down.

SF curves of seven different geometries at 293 Hz are plotted in figure 11. The curve shape is very similar to figure 10, but the SF values are lower. At 293 Hz the one-layer soldered paraboloid and two-layer soldered paraboloid shields provide the highest SF. All geometries have SF in the range of 90 - 98 % except for a three-layer soldered paraboloid magnetic shield with two sidewalls of soldered two-layer tape which has AC SF of 63 %. The lowest AC SF is given by the three-layer soldered paraboloid magnetic shield with two sidewalls two-layer soldered tape turned down in the range of 27 – 45 %. 293 Hz is a high enough frequency to generate additional AC losses in tapes causing local temperature increase and I_c reduction of the YBCO layer.

Figure 12 shows the frequency dependence of the SF for 1-3 layer soldered paraboloid shields (no sidewalls) at a magnetic field of 2 mT rms. For the one-layer magnetic shield, SF rises from 96 to 98 % in the 20 – 50 Hz frequency range. At higher frequencies, up to 293 Hz, SF is constant at a value of 98 %. The highest SF > 99.9 % was measured on the two-layer soldered shield at a frequency of 97 Hz. At higher frequencies up to 293 Hz, for a 2-3 layer shield, the SF drops due to the effect of magnetic relaxation, E(J) characteristic and local increase of AC losses in tapes.

A comparison of the measured SF for the one-layer soldered paraboloid shield with a 2D Comsol model of the same geometry and parameters at 20 and 293 Hz is presented in figure 13. SF measurements lay in the 95 – 98 % interval, 2D Comsol model results are in the 96.4 – 98.6 % interval. At 20 Hz and 6 mT, the SF difference between the 2D model and measurements is 1.1 %. For the 2D model, it is an acceptable difference since the curves of the same frequencies have a similar trend. 20 Hz curves are falling and 293 Hz curves are rising. The difference in slopes is caused by substrate μ_r frequency dependence because used YBCO tape has a magnetic substrate.

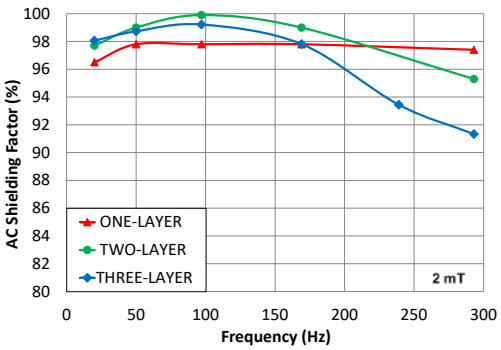

Figure 12. Measured SF frequency dependence for 1 - 3 layer soldered paraboloid shield, no sidewalls at 2 mT rms.

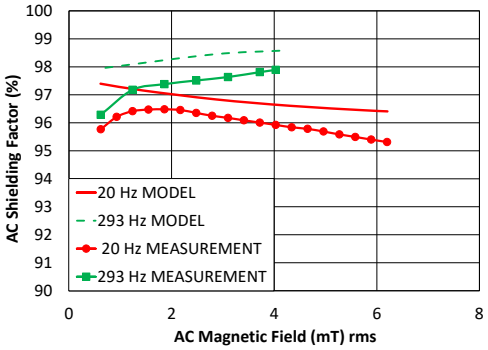

Figure 13. SF comparison of 2D simulation and experimental results for one-layer long paraboloid shield at frequencies 20 and 293 Hz.

5. Conclusion

The new measurement system for studying magnetic shielding of high-temperature superconductors of various shapes at cryogenic temperatures is described. A 40 cm bore copper magnet served as the noise source which was placed in stainless steel cryostat.

The shielding factors of 25 cm long paraboloid magnetic shields were measured at 77 K in a liquid nitrogen bath in DC and AC inhomogeneous magnetic fields at various frequencies.

Paraboloid magnetic shields were fabricated in one, two, and three-layer geometries using 45 mm wide edge soldered YBCO tapes. Shielding factors > 99 % were achieved at magnetic fields up to 7 mT at a frequency of 97 Hz with the two-layer soldered shield.

SF frequency dependencies in the two ranges 20 – 97 Hz and 97 – 338 Hz were observed. The shielding factors increase with increasing frequency in the range of 20 – 97 Hz at a constant external magnetic field. Silver, a highly conductive normal metal, and the magnetic substrate in the

superconducting tapes cause SF to increase with frequency. SF decreases in the 97 – 338 Hz range due to AC losses in the tapes increasing the temperature of the shield. We found out that the two-layer soldered configuration without side walls provided the highest shielding factor with low frequency dependence.

A 2D Comsol model was used for AC shielding factor calculations. We compared calculated and measured shielding factor data for the one-layer soldered shield and achieved a 1.1 % agreement.
In our future work, we will study the effect of lower temperatures in the useful long paraboloid structures and also in other geometries such as circular paraboloids.

The successful demonstration of high values of shielding factors > 99 % suggests that lightweight and thin magnetic shields could be produced with only a few layers of YBCO tapes for various applications. In this study, we concentrated on reducing the external magnetic field noise in the vicinity of a sensitive magnetic field sensor using an HTS 25 cm long paraboloid magnetic shield.

Acknowledgment
This work was supported by the Office of Naval Research through Grant N00014-16-1-2984, the authors would like to thank American Superconductor for providing the superconducting tape.

Appendix

In figures 14 and 15 we are showing the difference between unsoldered and soldered sidewalls to the bottom layers in the long paraboloid structure. Sidewalls were prepared from the same type of superconductor as bottom layers. The sample geometry description key is presented in figure 16.

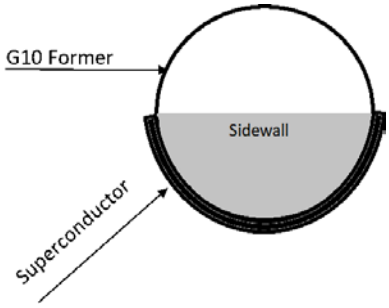

Figure 14. Long paraboloid structure with unsoldered sidewall.

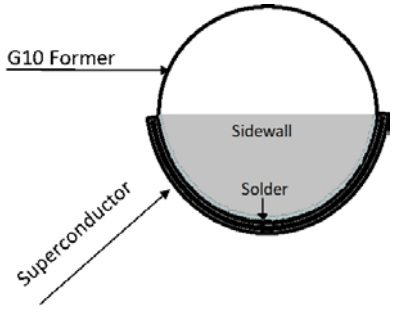

Figure 15. Long paraboloid structure with soldered sidewall. Please look to the solder in the corner between sidewall and bottom layer.

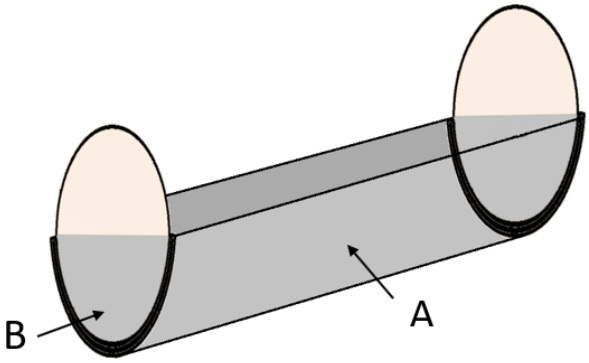

Figure 16. Sample geometry description key: A - number of soldered layers, B - sidewalls of several layers of unsoldered or soldered sidewalls to bottom tapes.

References

[1] Fagnard J-F, Elschner S, Bock J, Dirickx M, Vanderheyden B and Vanderbemden P 2010 Shielding efficiency and E(J) characteristics measured on large melt cast Bi-2212 hollow cylinders in axial magnetic fields *Supercond. Sci. Technol.* **23** 095012

[2] Fagnard J-F, Elschner S, Hobl A, Bock J, Vanderheyden B and Vanderbemden P 2012 Magnetic shielding properties of a superconducting hollow cylinder containing slits: modelling and experiment *Supercond. Sci. Technol.* **25** 104006

[3] Wéra L, Fagnard J F, Levin G A, Vanderheyden B, and Vanderbemden P 2013 Magnetic Shielding With YBCO Coated Conductors: Influence of the Geometry on Its Performances *IEEE Trans. Appl. Supercond.* **23** 8200504

[4] Tomków L, Ciszek M and Chorowski M 2015 Combined magnetic screen made of Bi-2223 bulk cylinder and YBCO tape rings—Modeling and Experiments *J. of Appl. Phys.* **117** 043901

[5] Wéra L, Fagnard J-F, Levin G A, Vanderheyden B and Vanderbemden P 2015 A comparative study of triaxial and uniaxial magnetic shields made of YBCO coated Conductors *Supercond. Sci. Technol.* **28** 074001

[6] Hogan K, Fagnard J-F, Wéra L, Vanderheyden B and Vanderbemden P 2018 Bulk superconducting tube subjected to the stray magnetic field of a solenoid *Supercond. Sci. Technol.* **31** 015001

[7] www.amsc.com

[8] Kvitkovic J, Voccio J, and Pamidi S V 2009 Shielding of AC magnetic fields by coils and sheets of superconducting Tapes *IEEE Trans. Appl. Supercond.* **19** 3577

[9] Kvitkovic J, Pamidi S and Voccio J 2009 Shielding AC magnetic fields using commercial YBa2Cu3O7-coated conductor tapes *Supercond. Sci. Technol.* **22** 125009

[10] Kvitkovic J, Patil P, Pamidi S V and Voccio J 2011 Characterization of 2G superconductor magnetic shields at 40–77 K *IEEE Trans. Appl. Supercond.* **21** 1477

[11] Kvitkovic J, Davis D, Zhang M and Pamidi S 2013 Influence of interlayer separation on magnetic shielding properties of 2G HTS sheets made of 46 mm wide RABiTS tape *IEEE Trans. Appl. Supercond.* **23** 8200605

[12] Kvitkovic J, Pamidi S, Graber L, Chiocchio T, Steurer M and Usoskin A 2014 AC Loss and Magnetic Shielding Measurements on 2GHTS Inductive Fault Current Limiter Prototype Modules *IEEE Trans. Appl. Supercond.* **24** 5600604

[13] Kvitkovic J, Davis D, Zhang M and Pamidi S 2015 Magnetic Shielding characteristics of second generation high temperature superconductors at variable temperatures obtained by cryogenic helium gas circulation *IEEE Trans. Appl. Supercond.* **25** 1

[14] Kvitkovic J, Hatwar R, and Pamidi S 2016 Simultaneous Magnetic Shielding and Magnetization Loss Measurements of YBCO Cylinders at Variable Temperatures Under Cryogenic Helium Gas Circulation *IEEE Trans. Appl. Supercond.* **26** 9000505

[15] Kvitkovic J, Patel S, and Pamidi S 2017 Magnetic Shielding Characteristics of Hybrid High-Temperature Superconductor/Ferromagnetic Material Multilayer Shields *IEEE Trans. Appl. Supercond.* **27** 4700705

[16] Kvitkovic J, Patel S, Zhang M, Zhang Z, Peetz J, Marney A and S. Pamidi S 2018 Enhanced Magnetic Field Sensing Using Planar High-Temperature Superconductor Shields *IEEE Trans. Appl. Supercond.* **28** 9001705

[17] Zhang M, Kvitkovic J, Kim J H, Kim C H, Pamidi S V, Coombs T A 2012 Alternating current loss of second-generation high-temperature superconducting coils with magnetic and non-magnetic substrate *Applied Physics Letters* **101** 102602

[18] Zhang Z, Kim J G, Kim C H, Pamidi S, Li J, Zhang M and Yuan W 2016 Current Distribution Investigation of a Laboratory-Scale Coaxial Two-HTS-Layer DC Prototype Cable *IEEE Trans. Appl. Supercond.* **26** 5400305

[19] www.arepoc.sk